Lawrence Berkeley National Laboratory

Lawrence Berkeley National Laboratory

Title

"Nanocrystal bilayer for tandem catalysis"

Permalink

https://escholarship.org/uc/item/15d0k5k2

Author

Yamada, Yusuke

Publication Date

2011-04-10

Peer reviewed

DISCLAIMER

This document was prepared as an account of work sponsored by the United States Government. While this document is believed to contain correct information, neither the United States Government nor any agency thereof, nor The Regents of the University of California, nor any of their employees, makes any warranty, express or implied, or assumes any legal responsibility for the accuracy, completeness, or usefulness of any information, apparatus, product, or process disclosed, or represents that its use would not infringe privately owned rights. Reference herein to any specific commercial product, process, or service by its trade name, trademark, manufacturer, or otherwise, does not necessarily constitute or imply its endorsement, recommendation, or favoring by the United States Government or any agency thereof, or The Regents of the University of California. The views and opinions of authors expressed herein do not necessarily state or reflect those of the United States Government or any agency thereof or The Regents of the University of California.

Nanocrystal Bilayer for Tandem Catalysis

Yusuke Yamada[1,3)], Chia-Kuang Tsung[1,2,4)], Wenyu Huang[1,2)], Ziyang Huo[1)], Susan E. Habas[1,2)], Tetsuro Soejima[1)], Cesar E Aliaga[2)], Gabor A. Somorjai[1,2)], Peidong Yang[1,2)]*

1. Department of Chemistry, University of California, Berkeley, Berkeley, California 94720, USA

2. Materials Sciences Division, Lawrence Berkeley National Laboratory, 1 Cyclotron Road, Berkeley, California 94720, USA

3. Current Address: Department of Material and Life Science, Graduate School of Engineering, Osaka University 2-1 Yamada-oka, Suita, Osaka 565-0871

4. Current Address: Department of Chemistry, Merkert Chemistry Center, Boston College, 2609 Beacon Street, Chestnut Hill, Massachusetts 02467, USA

*e-mail: p_yang@berkeley.edu

Supported catalysts have been widely used in industries and can be optimized by tuning the composition and interface of the metal nanoparticles and oxide supports. Rational design of metal-metal oxide interfaces in nanostructured catalysts is critical for achieving better reaction activities and selectivities. We introduce here a new class of nanocrystal tandem catalysts having multiple metal-metal oxide interfaces for the catalysis of sequential reactions. We utilized a nanocrystal bilayer structure formed by assembling sub-10 nm platinum and cerium oxide nanocube monolayers on a silica substrate. The two distinct metal-metal oxide interfaces, CeO_2-Pt and Pt-SiO_2, can be used to catalyze two distinct sequential reactions. The CeO_2-Pt interface catalyzed methanol decomposition to produce CO and H_2, which were then subsequently used for ethylene hydroformylation catalyzed by the nearby Pt-SiO_2 interface. Consequently, propanal was selectively produced on this nanocrystal bilayer tandem catalyst. This new concept of nanocrystal tandem catalysis represents a powerful approach towards designing high performance, multi-functional nanostructured catalysts.

High performance catalysts are central for the development of new generation energy conversion and storage technologies.[1,2] While industrial catalysts can be optimized empirically by tuning the elemental composition, changing the supports, or altering preparation conditions in order to achieve higher activity and selectivity, these conventional catalysts are typically not uniform in composition and/or surface structure at the nano- to micro-scale. In order to significantly improve our capability of designing better catalysts, new concepts for the rational design and assembly of metal-metal oxide interfaces are desired. Metal nanocrystals with well-controlled shape and size are interesting materials for catalyst design from both electronic structure and surface structure aspects.[3,4,5] From the electronic structure point of view, small metal nanoclusters have size-dependent electronic states, which make them fundamentally different from the bulk. From the surface structure point of view, the shaped nanocrystals have surfaces with well-defined atomic arrangements. It has been clearly demonstrated by surface science studies in recent decades that the atomic arrangement on the crystal surface can affect catalytic phenomena in terms of activity, selectivity, and durability.

The application of shape- and size-controlled metal oxide nanocrystals as catalyst supports has even greater potential for innovative catalyst design.[6,7] It is well known that catalysis can be modulated by using different metal oxide supports, or metal oxide supports with different crystal surfaces.[8] For example, platinum loaded molybdenum oxide and silica catalysts, both showed similar activation energies for ethylene hydrogenation.[9] On the other hand, the activation energy for ethane hydrogenolysis over platinum-silica was lower than that over platinum-molybdenum oxide.[10] It is believed that the metal oxides not only work as supports, but also function as electronic modulators, in addition to contributing spillover and adsorption sites. The precise selection and control of metal-oxide interfaces could lead to better activity and selectivity for a desired reaction.[11]

The integration of multiple types of metal-metal oxide interfaces on the surface of a single active metal nanocrystal could in principle yield a novel tandem catalyst for multi-step reactions. The catalytic activity and selectivity of such a tandem catalyst can be optimized by establishing suitable metal oxide interfaces for each reaction step. However, it is almost impossible to control the composition of multiple interfaces on an atomic level using traditional catalyst synthesis. Integrating binary nanocrystals to form highly ordered superlattice represents a new way to form multiple interfaces with new functionalities.[12,13] Here we utilized a nanocrystal bilayer structure formed by assembling sub-10 nm platinum and cerium oxide nanocube monolayers on a silica substrate. The two distinct metal-metal oxide interfaces in the catalyst, CeO_2-Pt and Pt-SiO_2, were used to catalyze two separate and sequential reactions. The CeO_2-Pt interface catalyzed methanol decomposition to produce CO and H_2 which were subsequently used for ethylene hydroformylation catalyzed by the nearby Pt-SiO_2 interface. Consequently, propanal was selectively produced on this nanocrystal bilayer tandem catalyst.

The cubic shape of nanocrystals is ideal for assembling metal-metal oxide interfaces with a large contact area. Figure 1 shows our tactic to achieve the "tandem" bilayer structure with nanocubes of metal and metal oxide. First, a two dimensional metal (Pt) nanocube array was assembled onto flat metal oxide substrate (SiO_2) by using Langmuir-Blodgett (LB) method to make the first metal-metal oxide interface. The second metal oxide (CeO_2) nanocube LB array was then assembled on top of the metal nanocube monolayer, which provides the second metal-metal oxide interface. The capping agents of the nanocrystals were removed by UV/ozone treatment to form clean metal-metal oxide interfaces.[20] After the capping agent removal, the vertical clefts between the nanocrystals assure access to both catalytic interfaces, while providing high surface area in the close packed array.

Olefin hydroformylation is an important reaction for the production of aldehydes from olefins, carbon monoxide, and hydrogen.[14] Usually the reaction is carried out with homogeneous catalysts, such as Rh complexes. The disadvantages of this process include the use of toxic CO and explosive H_2 gas. This process would also typically employ high pressure conditions and purification processes. Therefore, it would be advantageous to carry out olefin hydroformylation via heterogeneous catalysis with CO and H_2 produced *in situ* from the decomposition of a benign chemical, such as

methanol. It is known that Pt loaded on CeO_2 shows high activity toward methanol decomposition to provide CO and H_2.[15,16] In addition, Naito and Tanimoto reported that Pt loaded SiO_2 catalyzed propene hydroformylation and produced aldehydes with a high conversion rate. However, the selectivity for this reaction was poor.[17] Here, we demonstrate that our nanocrystal bilayer, made of a CeO_2 nanocube monolayer and Pt nanocube monolayer on a SiO_2 substrate, effectively catalyzes ethylene hydroformylation with methanol to produce propanal selectively.

Results and Discussions

Preparation of tandem catalyst Platinum and ceria nanocubes with edge lengths of 6-8 nm were prepared by literature methods with minor modifications.[18,19] A monolayer of platinum nanocubes was prepared by LB, and then transferred onto a Si wafer substrate with a native oxide layer on the surface. The original capping agent on the platinum nanocubes, tetradecyltrimethylammonium bromide (TTAB), was exchanged for oleylamine to facilitate LB assembly and deposition. The high resolution transmission electron microscopy (HRTEM) image of a single Pt nanocube and low magnification TEM images of a Pt LB film are shown in Figure 2a. The Pt nanocubes are single crystalline and enclosed by six (100) facets. The domain size of the monolayer film is over one micron by one micron, and the total coverage of the film was more than 80%. The gaps between the nanocrystals were about 2-3 nm, which are sufficient for diffusion of small molecules. The oleic acid capped CeO_2 nanocube monolayer film was prepared by drop casting or LB. Figure 2b shows a film prepared by drop casting. The gaps between the nanocrystals are 4-5 nm, which is close to the thickness of the oleic acid bilayer. The dropcast CeO_2 film showed long range ordering. For catalytic samples, the CeO_2 film was prepared by LB to give a large film area. The double-layered film was obtained by depositing a CeO_2 film onto a Pt film. A TEM image of a large area bilayered film of CeO_2 on Pt is shown in Figure 2c. Although the CeO_2 nanocrystals above the Pt nanocrystals cannot be clearly observed over most of the area due to their lower contrast, the CeO_2 nanocrystals were visible at some defect areas on the Pt film (Figure 3a). The presence of CeO_2 nanocubes on the Pt nanocube film was confirmed by HRTEM and by performing an energy dispersive X-ray (EDX) spectroscopy line scan as shown in Figure 3b and c. The Pt and CeO_2 lattice were both observed on the bilayer film by HRTEM (Figure 3b). The EDX line scan over the defect area of the bilayer film is shown in Figure 3c. It shows the intensity change of Pt and Ce along the line on the film where the Pt film is discontinuous. The Pt intensity decreases at the gap between Pt nanocrystals while the Ce intensity was nearly constant.

In order to facilitate interface formation between the SiO_2, Pt, and CeO_2 layers, the various capping agents, oleylamine on Pt and oleic acid on CeO_2, need to be removed. Although CeO_2 crystals are stable under high temperature treatment for capping agent removal, Pt nanocubes are not stable under such conditions. When Pt nanocrystal loaded samples were heated at 250°C in air, the shape of the Pt nanocrystals was lost. Thus, we applied a room temperature UV-irradiation process to remove surface capping agents. Previously, it was found that UV/ozone treatment is effective for removing organic capping agents from Pt nanoparticles.[17] Here, removal of the capping agent was monitored by sum frequency generation vibrational spectroscopy as shown in Figure S1 (Supporting information). Before the UV/ozone treatment, three peaks assigned to symmetric CH_2 (2853 cm^{-1}), symmetric CH_3 (2879 cm^{-1}), and asymmetric CH_2 (2929

cm^{-1}) stretches, were observed. After treatment, the intensity of the peaks was significantly decreased. TEM observations of the sample before and after the UV/ozone treatment indicated that the crystal shapes remained unchanged. Oxidation of CO is commonly employed to examine the interaction between Pt and metal oxides because the activation energy of Pt loaded on a metal oxide is highly dependent on the nature of metal oxide support.[21,22,23] The strong Pt-metal oxide interaction decreases electron donation from Pt to adsorbed CO weakening the CO bond. As the result, the interaction between Pt and the metal oxide increases the activation energy for CO oxidation. Arrhenius plots for CO oxidation over our CeO_2-Pt bilayers on SiO_2 substrates before and after UV/ozone treatment are shown in Figure S2. The as-prepared bilayers showed an apparent activation energy of 19.7 kcal/mol which is comparable to the reported value of Pt nanocubes.[22] The UV/ozone treated samples showed an apparent activation energy of 30.1 kcal/mol. The increase in activation energy indicates the formation of two metal-metal oxide interfaces of CeO_2-Pt and Pt-SiO_2 following capping agent removal.

Ethylene hydroformylation over tandem catalyst with MeOH The assembly of CeO_2-Pt-SiO_2 bilayers with two different metal-metal oxide interfaces is an ideal catalyst design for olefin hydroformylation with CO and H_2 formed *in situ* by the decomposition of MeOH. It was reported previously that Pt/CeO_2 can selectively catalyze MeOH decomposition to CO and H_2, while Pt/SiO_2 catalyzes olefin hydroformylation. Prior to examining the two-step tandem reaction, control experiments were performed to monitor each step over each interface individually: MeOH decomposition over the Pt/CeO_2 interface, and then separately ethylene hydroformylation with CO and H_2 gas input over the Pt/SiO_2 interface. The decomposition of MeOH over the Pt/CeO_2 interface was examined at 190 °C over Pt-CeO_2-SiO_2 catalyst, which contains only of Pt/CeO_2 - metal/oxide interface. The as-prepared catalyst showed no catalytic activity for the reaction due to the lack of clean metal-metal oxide interfaces (Figure S3). After UV/ozone treatment, the Pt-CeO_2-SiO_2 tandem catalyst showed MeOH decomposition activity as shown in Figure 4a. The concentration of formed hydrogen and decomposed MeOH in the batch reactor changed in proportion to the reaction time and the ratio of formed H_2 to decomposed MeOH is 1:2, which confirms the formation of H_2 and CO. The turn over frequency, TOF, in terms of H_2 was 1.8×10^{-3} s^{-1} per Pt atom. Separately, ethylene hydroformylation with CO and H_2 gas was carried out over the Pt-SiO_2 catalyst also at 190 °C. Figure 4b shows the concentration change of propanal and MeOH in a batch rector as a function of the reaction time. The propanal formation was clearly observed. The production of MeOH was due to the hydrogenation of CO, which was confirmed by CO hydrogenation with only CO and H_2 without ethylene (Figure S4). The TOF in terms of MeOH was 5.8×10^{-2} s^{-1} per Pt atom and the TOF in terms of propanal was 2.7×10^{-3} s^{-1} per Pt atom. On a bare Pt surface, the formation of MeOH by CO hydrogenation is much faster than propanal formation by hydroformylation.

Figure 5a shows time dependent propanal formation from ethylene hydroformylation with *in situ* MeOH decomposition over the CeO_2-Pt-SiO_2 tandem catalyst at 190 °C. The as-prepared sample produced a negligible amount of propanal even after a longer reaction time (Figure S3). On the other hand, the formation of propanal was clearly observed over the UV/ozone treated catalyst as shown in Figure 5a. Propanal formation over the UV/ozone treated catalyst was further

confirmed by a mass spectroscopy and quantified by gas chromatography (Figure S5). The formation of by-products such as propanol or ethane was less than the detection limit (<0.01 vol%). The maximum propanal concentration in the reaction effluent was 0.18% where the product selectivity toward propanal was more than 94%. This is quite surprising since simple ethylene hydrogenation, a competitive reaction of hydroformylation, is much faster on conventional Pt catalysts. The same reaction over the $Pt-CeO_2-SiO_2$ catalyst, which doesn't contain the suitable interfaces for the reaction, was also performed as a control experiment. No formation of propanal was observed.

Hydroformylation with *in situ* decomposition of MeOH over the tandem $CeO_2-Pt-SiO_2$ catalyst gave a TOF for propanal of 2.6×10^{-2} s^{-1} per Pt atom, which was much faster than that obtained for ethylene hydroformylation with CO and H_2 gas over the $Pt-SiO_2$ catalyst. Two reasons for the better performance of the tandem catalyst are proposed here. First, for the *in situ* tandem catalytic reaction, MeOH decomposition occurred preferentially at the $Pt-CeO_2$ interface while the rate of MeOH formation by CO hydrogenation is significantly decreased because of the high MeOH concentration. The high density of CO and hydrogen at the Pt surface is also beneficial for ethylene hydroformylation. Secondly, it is also possible that the electronic effects of CeO_2 contribute to fundamentally change the catalytic properties of the $Pt-SiO_2$ interface for more efficient hydroformylation.

In order to demonstrate the unique properties of our tandem catalysts, the same catalytic reactions were also examined over physical mixtures of Pt/CeO_2 and Pt/SiO_2 prepared by a conventional impregnation method. The Pt concentration was changed from 1 to 5 wt% for both catalysts. These physical mixture catalysts always produced ethane as a primary product and small amount of propane, which is likely to be formed by the successive hydrogenation of propanal (Figure S6). At the mixture of $3\%Pt/SiO_2$ and $3\%Pt/CeO_2$, the TOF of propane formation was 5.7×10^{-4} s^{-1} per Pt atom, which is much slower than the TOF of propanal formation, 2.6×10^{-2} s^{-1} per Pt atom, over the tandem catalyst. The different catalytic behaviors between the tandem catalyst and mixture catalysts clearly demonstrated the designed interfaces in our tandem catalysts can be used to program sequential chemical reactions effectively.

The novel concept of a nanocrystal bilayer "tandem catalyst" involves multiple distinct metal-metal oxide interfaces corresponding to specific catalytic activities and selectivities. This concept was tested using a CeO_2/Pt nanocube bilayer structure with well-defined surface structures on a silica substrate. Ethylene hydroformylation with hydrogen and carbon monoxide formed *in situ* by MeOH decomposition was demonstrated. Sequential chemical reactions at two different neighboring metal-metal oxide interfaces acted to selectively produce propanal. While tandem catalysis has been previously employed in homogenous catalytic systems,[24,25] the current study represents the first such attempt using rationally designed and assembled nanocrystal bilayers with multiple built-in metal-metal oxide interfaces. This new concept of nanocrystal tandem catalysis represents a powerful approach towards designing high performance, multi-functional nanostructured catalysts for multiple-step chemical reactions such as those proposed for artificial photosynthesis.

Methods

Platinum and ceria nanocubes synthesis.

Platinum nanocubes and ceria nanocubes were prepared by reported methods with minor modifications.[18,19]

An aqueous solution of K_2PtCl_4 (10 mM, 1 mL) was added to an aqueous solution of trimethyltetradecylammonium bromide (TTAB, 119 mM, 8.4 mL). After vigorous stirring, the solution was left at room temperature until a white crystalline solid formed. Then the mixture was heated at 50 °C with magnetic stirring until a clear solution was achieved. To the solution was added an ice cold aqueous solution of $NaBH_4$ (500mM, 0.6 mL). Excess hydrogen formed during the first 15 min was released through a needle. The solution was stirred for more than 6 hours. The crude product was purified by discarding the precipitate following centrifugation at 3000 rpm for 30 min. The procedure was repeated four times. The shape of particles was observed by a Tecnai 12 Transmission electron microscope or Tecnai G2 S-Twin.

Oleylamine coated Pt nanocubes were obtained by performing ligand exchange on the purified Pt nanocubes described above. Platinum nanocubes capped with TTAB were collected by centrifugation at 14,000 rpm for 30 min. The resulting powder (1.8×10^{-5} mol Pt, nominal) was then washed with deionized water twice and re-dispersed in water and oleylamine (61 mol20 L). The suspension was heated at 50 °C overnight with magnetic stirring. The slurry was then washed with methanol and a chloroform methanol mixture several times before re-dispersing the particles in $CHCl_3$.

Cerium oxide nanocubes were prepared by autoclave at high temperature.[19] Hydrochloric acid (50 L), toluene (15 mL), oleic acid (1.5 mL) and *tert*-butylamine (0.15 mL) were added to an aqueous solution of cerium nitrate hexahydrate (16.7 mM, 15 mL) in a Teflon cup (45 mL inner volume). The Teflon cup was sealed in a stainless steel jacket and heated to 180 °C for 24 hours. The organic phase was collected and purified by centrifugation at 3000 rpm for 5 min. The particles were precipitated by addition of double the volume of ethanol, followed by centrifugation at 14,000 rpm for 10 min to isolate the yellowish white powder. The powder was washed twice with a hexane-ethanol mixture.

LB film preparation.

Platinum LB films were prepared with oleylamine-capped Pt nanocubes. Following ligand exchange and washing, the Pt-oleylamine particles were re-dispersed in chloroform (0.5 mL). The solution was slowly dropped onto a water subphase on a LB trough. After evaporation of the chloroform over 30 min, the film was compressed until a surface pressure of 10-15 mN/m was achieved. The resulting film was aged for 30 min and then transferred onto a Si substrate. Ceria nanocube LB films were prepared as the same manner with a chloroform solution of ceria nanocubes. HRTEM images and EDX spectra were recorded on a Philips CM200.

Catalysis measurements.

All catalysis measurements were carried out with a closed circulation set up. A Si wafer loaded with the nanocube bilayer film was loaded into a glass tube with an inner diameter of 11 mm. A stream of N_2 gas was passed over the sample,

which was then heated to the desired temperature for measurement. The temperature was monitored with a thermocouple inserted into a glass sheath placed onto the sample. After the temperature stabilized, the reaction gas of 40 torr CO, 100 torr O_2 and 620 torr N_2 was introduced into the reaction chamber to examine CO oxidation catalysis. The reaction products were quantified approximately every 30 min by a gas chromatograph with two columns and TCD detectors. A Molecular Sieve 5A column with Ar carrier gas was used for quantification of O_2, N_2 and CO, and a Poraplot Q column with He carrier gas was used for CO_2 quantification. The number of Pt atoms exposed to the reaction gas was estimated from SEM images. The MeOH decomposition reaction was carried out in a similar manner. N_2 gas with 30 torr MeOH was introduced into the reaction chamber with the catalyst. H_2 produced by the catalytic reaction was separated and quantified by the Molecular Sieve 5A column. Hydroformylation was performed with a gas mixture of 7.6 torr ethylene, 30 torr CO, 30 torr H_2 and 692 torr N_2. Product analysis was performed every 2 hours. Propanal formed during the reaction was separated and quantified with a Poraplot Q column. Ethylene hydroformylation with H_2 and CO formed *in situ* by methanol decomposition was investigated with a gas mixture of 7.6 torr ethylene, 30 torr MeOH and 722 torr N_2. The estimation of turnover frequency was based on the number of Pt atoms on the surface of nanoparticles.

Author Contributions

Y.Y., C.T., G.S. and P.Y. conceived and designed the experiments. Y.Y., W.H. and C. A. performed the experiments. Z.H., S.H., T.S. and C. A. contributed materials and analysis tools. Y.Y., C. T., W.H. and P. Y. co-wrote the paper. All authors discussed the results and commented the manuscript.

References

1   Centi, G. & Perathoner, S. Catalysis: Role and Challenges for a Sustainable Energy. *Top. Catal.* **52**, 948-961 (2009).

2   Norskov, J. K., Bligaard, T., Rossmeisl, J. & Christensen, C. H. Towards the Computational Design of Solid Catalysts. *Nat. Chem.* **1**, 37-46 (2009).

3   Ott, L. S. & Finke, R. G. Transition-metal Nanocluster Stabilization for Catalysis: A Critical Review of Ranking Methods and Putative Stabilizers. *Coord. Chem. Rev.* **251**, 1075-1100 (2007).

4   Somorjai, G. A., Frei, H. & Park, J. Y. Advancing the Frontiers in Nanocatalysis, Biointerfaces, and Renewable Energy Conversion by Innovations of Surface Techniques. *J. Am. Chem. Soc.* **131**, 16589-16605 (2009).

5   Somorjai, G. A., Tao, F. & Park, J. Y. The Nanoscience Revolution: Merging of Colloid Science, Catalysis and Nanoelectronics. *Top. Catal.* **47**, 1-14 (2008).

6   Si, R. & Flytzani-Stephanopoulos, M. Shape and Crystal-plane Effects of Nanoscale Ceria on the Activity of Au-CeO$_2$ Catalysts for the Water-gas Shift Reaction. *Angew. Chem. Int. Ed.* **47**, 2884-2887 (2008).

7   Xie, X. W., Li, Y., Liu, Z. Q., Haruta, M. & Shen, W. J. Low-temperature Oxidation of CO Catalysed by Co$_3$O$_4$ Nanorods. *Nature* **458**, 746-749 (2009).

8   Stakheev, A. Y. & Kustov, L. M. Effects of the Support on the Morphology and Electronic Properties of Supported Metal Clusters: Modern Concepts and Progress in 1990s. *Appl. Catal. , A* **188**, 3-35 (1999).

9   Jackson, S. D. *et al.* Supported Metal Catalysts: Preparation, Characterization, and Function .5. Activities and Selectivities of Platinum Catalysts in the Reactions of Cyclopropane, Ethene, 1,3-Butadiene, and 2-Butyne with Dihydrogen. *J. Catal.* **162**, 10-19 (1996).

10   Jackson, S. D., Kelly, G. J. & Webb, G. Supported Metal Catalysts; Preparation, Characterisation, and Function - Part VI. Hydrogenolysis of Ethane, Propane, *n*-Butane and *iso*-Butane over Supported Platinum Catalysts. *J. Catal.* **176**, 225-234 (1998).

11   Zhou, Z., Kooi, S., Flytzani-Stephanopoulos, M. & Saltsburg, H. The Role of the Interface in CO Oxidation on Au/CeO$_2$ Multi-Layer Nanotowers. *Adv. Funct. Mater.* **18**, 2801-2807 (2008).

12   Shevchenko, E. V., Talapin, D. V., Kotov, N. A., O'Brien, S. & Murray, C. B. Structural Diversity in Binary Nanoparticle Superlattices. *Nature* **439**, 55-59 (2006).

13   Urban, J. J., Talapin, D. V., Shevchenko, E. V., Kagan, C. R. & Murray, C. B. Synergism in Binary Nanocrystal Superlattices Leads to Enhanced *p*-Type Conductivity in Self-assembled PbTe/Ag$_2$Te Thin Films. *Nat. Mater.* **6**, 115-121 (2007).

14   Ungvary, F. Hydroformylation - Homogeneous in *Encyclopedia of Catalysis* Vol. 3 (ed Istvan T. Horvath) (John Wiley & Sons, Inc., 2003).

15   Croy, J. R. *et al.* Support Dependence of MeOH Decomposition over Size-selected Pt Nanoparticles. *Catal. Lett.* **119**, 209-216 (2007).

16   Imamura, S. *et al.* Decomposition of Methanol on Pt-loaded Ceria. *Catal. Today* **50**, 369-380 (1999).

17   Naito, S. & M., T. Effect of Sodium Cation Addition on the Hydroformylation of Propane over Silica-supported Group VIII Metal Catalysts. *J. Chem. Soc. Chem. Commun.*, 1403-1404 (1989).

18   Lee, H. *et al.* Morphological Control of Catalytically Active Platinum Nanocrystals. *Angew. Chem. Int. Ed.* 45, 7824-7828 (2006).

19   Yang, S. & Gao, L. Controlled Synthesis and Self-Assembly of CeO_2 Nanocubes. *J. Am. Chem. Soc.* **128**, 9330-9331 (2006).

20   Aliaga, C. *et al.* Sum Frequency Generation and Catalytic Reaction Studies of the Removal of Organic Capping Agents from Pt Nanoparticles by UV-Ozone Treatment. *J. Phys. Chem. C* **113**, 6150-6155 (2009).

21   Contreras, A. M., Yan, X.-M., Kwon, S., Bokor, J. & Somorjai, G. A. Catalytic CO Oxidation Reaction Studies on Lithographically Fabricated Platinum Nanowire Arrays with Different Oxide Supports. *Catal. Lett.* **111**, 5-13 (2006).

22   Kweskin, S. J. *et al.* Carbon Monoxide Adsorption and Oxidation on Monolayer Films of Cubic Platinum Nanoparticles Investigated by Infrared-visible Sum Frequency Generation Vibrational Spectroscopy. *J. Phys. Chem. B* **110**, 15920-15925 (2006).

23   Panagiotopoulou, P. & Kondarides, D. I. A Comparative Study of the Water-gas Shift Activity of Pt Catalysts Supported on Single (MOx) and Composite (MOx/Al_2O_3, MOx/TiO_2) Metal Oxide Carriers. *Catal. Today* **127**, 319-329 (2007).

24   Wasilke, J. C. *et al.*   Concurrent Tandem Catalysis. *Chem. Rev.* **105**, 1001-1020 (2005).

25   Felpin, F. X. & Fouquet, E.   Heterogeneous Multifunctional Catalysts for Tandem Processes: An Approach toward Sustainability. *Chem. Sus. Chem.* **1**, 718-724 (2008).
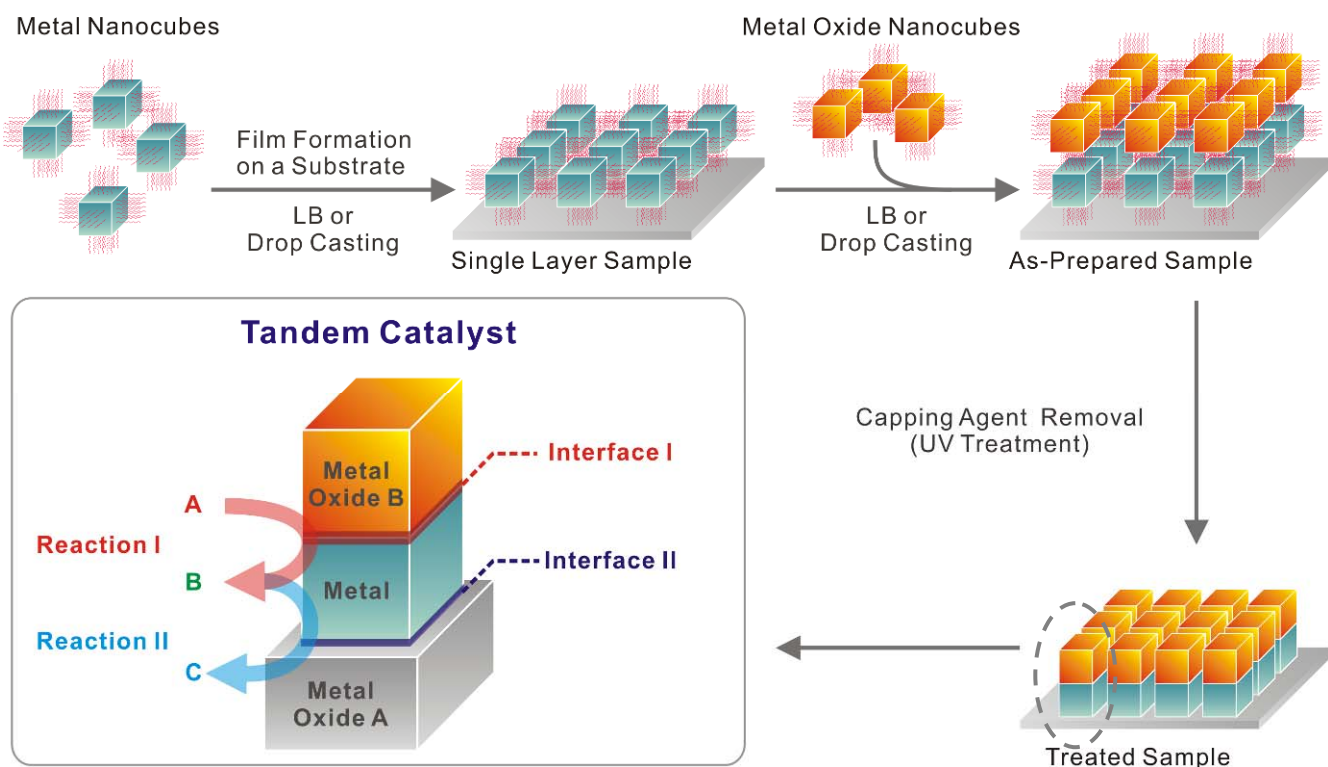
Figure 1. Schematic illustration of the assembly process for the preparation of nanocrystal bilayer "tandem catalyst". Single layers of metal nanocubes and metal oxide cubes were deposited sequentially. Capping agents of nanoparticles were removed by UV treatment.
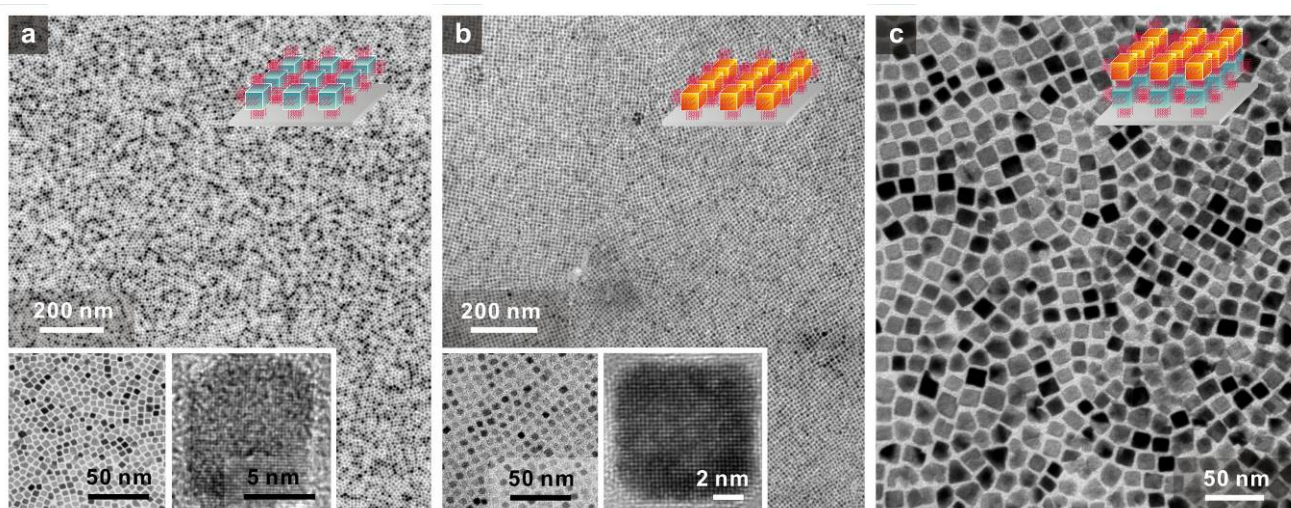

FFigure 2. Monolayer films of Pt nanocubes and CeO_2 nanocubes and bilayer film of CeO_2-Pt nanocubes observed by TEM. (a) a Pt film prepared by Langmuir-Blodgett technique, (b) a CeO_2 nanocube assembly prepared by drop casting and (c) a CeO_2 nanocube monolayer on a Pt monolayer. The inset figures are the TEM images of higher magnification and an HRTEM image of a single nanocrystal.
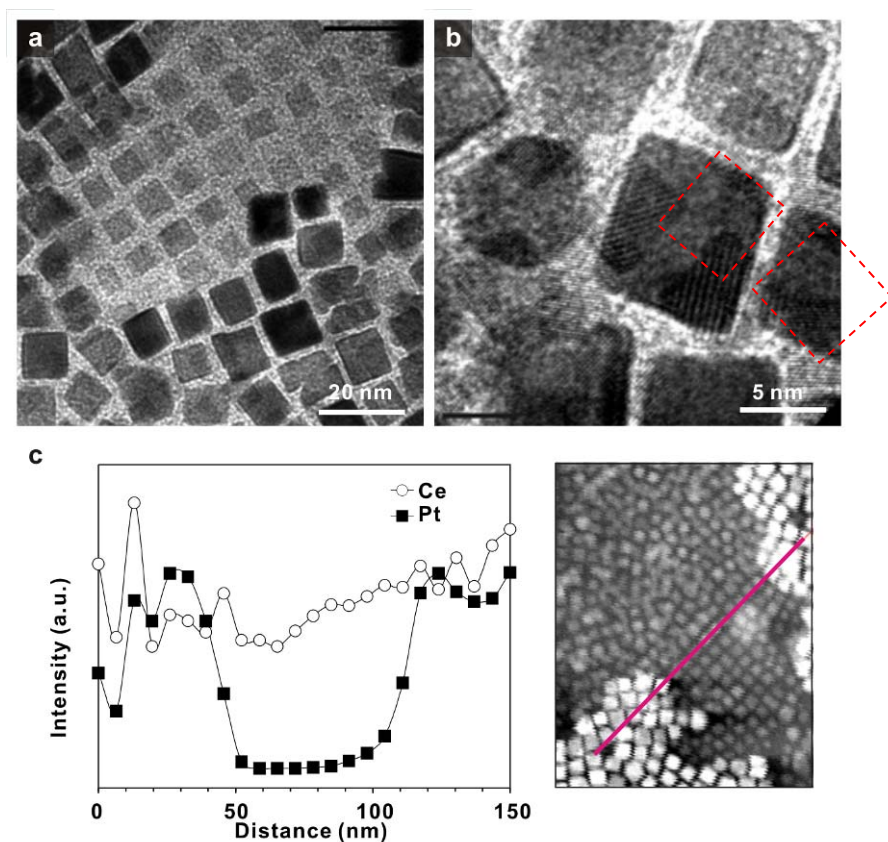
Figure 3. Nanocrystals bilayer observed by HR TEM and EDX. (a) A TEM image of a defective area of a bilayer film, (b) A HRTEM image showing the overlapping CeO$_2$/Pt nanocubes and (c) EDX line profile at the defective area of a bilayer film. The line profile was collected along the red trace in the image.
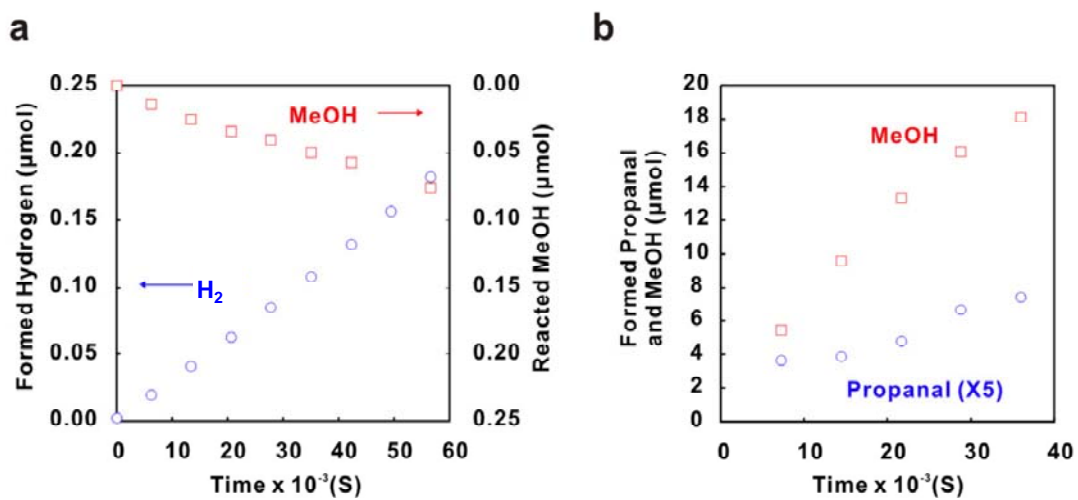
Figure 4. MeOH decomposition over Pt/CeO_2 and conventional hydroformylation over Pt/SiO_2. (a) Hydrogen produced as a function of reaction time over Pt on CeO_2 at 190 °C by catalytic thermal decomposition of methanol (open circle; formed hydrogen, open square; decomposed MeOH) (b) Propanal and MeOH produced as a function of reaction time over Pt nanocube on SiO_2 nanocube at 190°C from ethylene, carbon monoxide and hydrogen. (open square; MeOH, open circle; propanal)
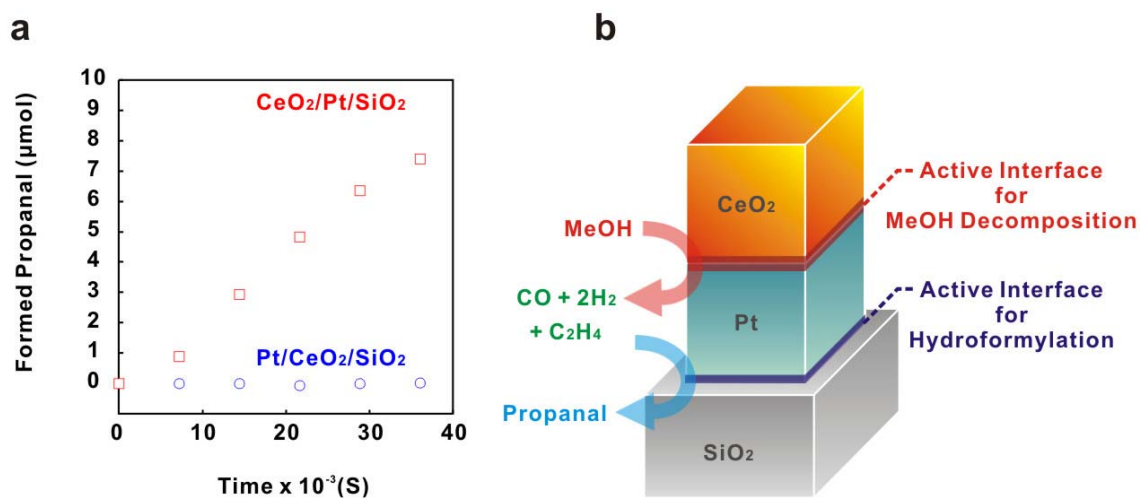
Figure 5. Ethylene hydroformylation with MeOH over tandem catalyst. (a) Propanal produced as a function of reaction time over CeO_2-Pt-SiO_2 and Pt-CeO_2-SiO_2 bilayer at 190°C from ethylene and MeOH. (open square; CeO_2-Pt-SiO_2, open circle; Pt-CeO_2-SiO_2) (b) Schematic drawing of the CeO_2-Pt-SiO_2 tandem catalyst.